

Cluster and Periodic DFT Calculations of MgO/Pd(CO) and MgO/Pd(CO)₂ Surface Complexes

Annalisa Del Vitto, Livia Giordano, and Gianfranco Pacchioni*

Dipartimento di Scienza dei Materiali, Università Milano-Bicocca, via R. Cozzi 53, I-20125 Milano, Italy

Ulrich Heiz

Departement Chemie, Technische Universität München, Lichtenbergstrasse 4, 85747 Garching, Germany

Received: November 3, 2004; In Final Form: December 9, 2004

The bonding and vibrational properties of Pd(CO) and Pd(CO)₂ complexes formed at the (100) surface of MgO have been investigated using the gradient-corrected DFT approach and have been compared to the results of infrared and thermal desorption experiments performed on ultrathin MgO films. Two complementary approaches have been used for the calculation of the electronic properties: the embedded cluster method using localized atomic orbital basis sets and supercell periodic calculations using plane waves. The results show that the two methods provide very similar answers, provided that sufficiently large supercells are used. Various regular and defect adsorption sites for the Pd(CO) and Pd(CO)₂ have been considered: terraces, steps, neutral and charged oxygen vacancies (F and F⁺ centers), and divacancies. From the comparison of the computed and experimental results, it is concluded that the most likely site where the Pd atoms are stabilized and where carbonyl complexes are formed are the F⁺ centers, paramagnetic defects consisting of a single electron trapped in an anion vacancy.

1. Introduction

Size-selected metal atoms and clusters on oxide surfaces represent well-defined models of more complex heterogeneous catalysts.¹ The properties of the deposited nanoclusters depend on various factors like cluster size, the oxide substrate, the presence of point and extended defects, and so forth.^{2–4} A detailed characterization of the sites where metal particles are stabilized at the surface of oxide single crystals or thin films is thus essential to identify structure–property relationships. One of the systems which has been studied in greater detail are Pd and Au atoms and clusters deposited on MgO thin films.^{1–4} From several measurements, it appears that point defects at the surface of MgO play an important role in trapping the metal atoms and in promoting the catalytic activity of the metal clusters.^{2,3} In this respect, a special effort has been done to identify the point defects most likely involved in the nucleation and growth of metal nanoclusters.^{5,6}

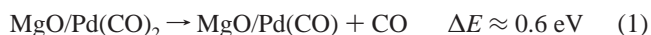
The number of potential candidates as trapping sites at the surface of MgO is quite large,⁷ and it is only through a careful comparison of experimental measurements and computational simulations that one can gain direct insight into the problem. Recently, we have shown that the properties of CO molecules adsorbed on MgO-supported Pd atoms can be very useful to identify the surface sites where the atoms are bound.^{8–10} To this end, Pd atoms have been deposited on the MgO surface at low temperature and with low kinetic energy to avoid surface damage in the deposition step. Accurate calculations show that the diffusion barrier for Pd atoms on MgO terraces is relatively low (0.34 eV),⁹ so that even at the deposition temperature the atoms possess enough residual kinetic energy to diffuse on the surface until they become trapped at a specific point defect.

When CO is dosed at low temperature in the UHV chamber, it binds to the supported Pd atoms more strongly than to the MgO cation sites, thus titrating selectively the metal atoms.

From the study of thermal desorption (TDS) and infrared (IR) spectra, one can obtain direct information on the PdCO binding energies and vibrational frequencies.^{8,9} In a first study,⁸ it was found that CO desorbs from the Pd₁/MgO surface at a temperature of about 260 K; using a Redhead analysis of the TDS spectrum and a preexponential factor of 10¹³ s^{−1}, a desorption energy of 0.7 ± 0.1 eV has been obtained. In a more recent study,⁹ it has been possible to detect also a second peak at 370 K, corresponding to a desorption energy of ≈1.0 eV. In this new experiment, the first desorption temperature occurs around 230 K and corresponds to a Pd–CO binding of ≈0.6 eV.

The vibrational analysis performed using ¹³CO molecules has shown that the Pd atoms can bind two CO molecules, forming MgO/Pd(CO)₂ complexes with vibrational frequencies at 2010 and 2045 cm^{−1}.^{8,9} By heating the sample to about 250 K, one CO molecule desorbs from the complex, leaving on the surface a PdCO molecule. The corresponding frequency is 2010 cm^{−1} and has been attributed to a single CO molecule bound to a Pd atom. Considering an isotopic shift of about 45 cm^{−1} going from ¹³CO to ¹²CO, the expected ¹²CO vibrational frequencies are at 2055 and 2090 cm^{−1} for MgO/Pd(CO)₂ and at 2055 cm^{−1} for MgO/Pd(CO).

Thus, two CO desorptions occur from Pd₁/MgO:



Another intense peak at 120 K arises from CO bound at MgO defects, probably steps.^{8,9}

* Corresponding author. E-mail: gianfranco.pacchioni@unimib.it.

The results have been interpreted by means of cluster model DFT calculations using the gradient-corrected hybrid B3LYP exchange-correlation functional.^{8–10} The sites considered are surface or low-coordinated oxide anions, O^{2–}, and oxygen vacancies, F_{5c} or F_{5c}⁺ centers (5c = five-coordinated). The results have shown that the measured CO desorption energies are incompatible with the hypothesis that the Pd atoms are bound to oxide anions: in this case, the calculated Pd–CO binding energies should be of 2–3 eV, that is, ≈ 3 times larger than the measured ones, 0.6–1.0 eV. On the other hand, Pd–CO binding energies of less than 1 eV are consistent with Pd atoms bound at F_{5c} or F_{5c}⁺ centers, thus providing a strong support to the hypothesis that these are the sites where the metal atoms are stabilized. The computed CO vibrational frequencies, however, have been considered less reliable because of the presence of a nonuniform electric field generated in embedded clusters by the point charges used to reproduce the Madelung potential of the extended solid.^{9,10}

In this study, we have reconsidered the problem of the properties of MgO/Pd(CO) and MgO/Pd(CO)₂ complexes using two different approaches and considering new adsorption sites for Pd which have not been included in the previous studies. The new sites are oxide anions at monoatomic steps (the previous calculations have been done for edge sites) and MgO divacancies, V_{MgO} (a divacancy consists of a pair of Mg and O missing ions).^{11,12} Divacancies are likely present on the surface of freshly cleaved MgO single crystals,¹³ have a lower formation energy than single vacancies,¹¹ and have been proposed as potential sites for nucleation and growth of metal clusters from aggregation of isolated atoms.¹⁴ In this respect, the present study fills a hole in the map of MgO surface defects potentially involved in the trapping of metal atoms.

The second new aspect of the study is that the cluster calculations have been performed using a more accurate embedding procedure which includes in the calculations the long-range electronic polarization of the surface through a shell model approach.¹⁵ The same properties have been computed with a completely different approach based on supercell plane wave calculations using the VASP code.¹⁶ The same exchange-correlation functional has been used for cluster and periodic calculations (see below). In this way, the properties of the PdCO complexes are determined with two different but complementary approaches, and the most important MgO sites potentially involved in Pd adsorption are treated on the same footing providing a consistent set of data to compare with the experiment.

2. Computational Details

The calculations are based on gradient-corrected density functional theory (DFT) using cluster models and periodic supercell approaches. In the first case, the MgO surface is represented by a large cluster. The system consists of a quantum-mechanical part (QM) treated at the DFT level using the generalized-gradient approximation (GGA) form of the exchange-correlation functional proposed by Perdew and Wang (PW-91);¹⁷ the QM part is surrounded by interface Mg* ions described by an effective core potential (ECP)¹⁸ and by a region of about 900 polarizable classical shell model ions. All QM and interface ions are fully relaxed. For some specific defects (divacancies and F_{5c}⁺ centers), the position of the shell model ions has also been optimized, thus including the geometrical relaxation in a large region around the defect. The cluster is embedded in an array of $\gg 3200$ classical ions fixed at the bulk lattice positions which reproduce the long-range electrostatic potential. The size

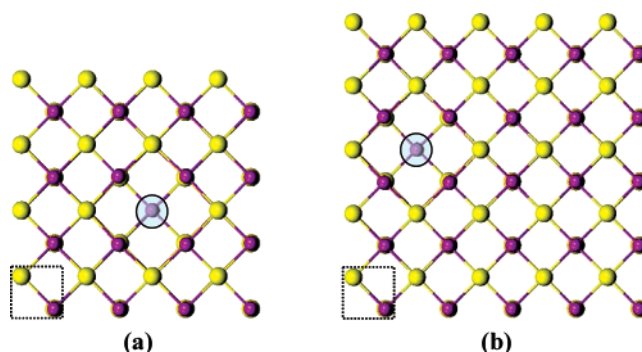


Figure 1. (a) Top view of the 4×4 and (b) top view of the 5×5 supercells used in periodic calculations. The circle indicates the atom removed to create an oxygen vacancy.

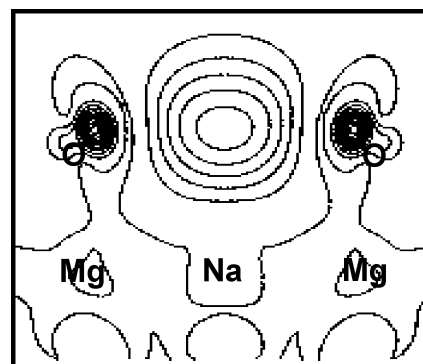


Figure 2. Electron spin density of a F_{5c}⁺ center as described by a Na-doped MgO supercell with an oxygen vacancy. The plot is for a plane normal to the surface.

of the QM part is Mg₁₃O₁₄Mg*₁₇ for a terrace and Mg₁₃O₁₃Mg*₁₇ for a step site. This hybrid scheme is implemented in the GUESS code¹⁹ interfaced with Gaussian98.²⁰ Linear combinations of atomic orbital (LCAO), all-electron 6-31G basis sets have been used for the Mg and O atoms of the QM cluster, while for Pd we used a small-core ECP and a lan12dz basis set with the s and d shells partially decontracted;²¹ the C–O molecule has been treated with a 6-311+G* basis set which includes both diffuse and polarization functions. The cluster results have been corrected for the basis set superposition error (BSSE) using the standard counterpoise correction.²²

The MgO/PdCO interaction has also been studied with periodic supercell calculations using a plane wave basis set (kinetic energy cutoff at 396 eV), ultrasoft pseudopotentials,²³ and the same PW-91 exchange-correlation functional used for the cluster calculations.¹⁷ For the periodic calculations, we used the VASP code.¹⁶ The MgO(100) surface has been modeled by three MgO layers; during geometry optimization, all atoms in the two surface nearest layers were relaxed while the atoms in the third layer were frozen at bulk positions. The atoms within the supercell are relaxed until the average atomic forces are less than 0.01 eV/Å. The calculations have been performed at the Γ point using 4×4 supercells containing 96 Mg and O atoms. In selected cases, a 5×5 supercell containing 150 Mg and O atoms, Figure 1, has also been considered (see below). For the step, we used a (510) surface. The charged F⁺ surface center is difficult to treat in a periodic calculation because of the problems connected with the supercell background neutralization. However, models of paramagnetic F centers can be obtained in periodic calculations by doping the surface with H²⁴ or Na²⁵ atoms. Here, we adopted the second procedure, and we replaced the Mg atom at the bottom of the vacancy with a Na atom, thus introducing a hole in the system. The unpaired

TABLE 1: Properties of a CO Molecule Adsorbed on a Pd Atom Stabilized at Various Sites of the MgO(100) Surface: Cluster and Periodic 4×4 Supercell Results^f

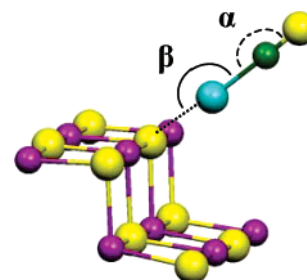
		free ^a	terrace	step	V_{MgO}	F_{5c}	F_{5c}^+	
$d(\text{S-Pd})$, Å	cluster		2.101	2.176	2.233	2.675	2.727	
	periodic		2.086	2.201	2.239	2.657	2.76	
CO orientation			normal	normal	tilted	tilted ^b	normal	normal
$d(\text{S-PdCO})$, Å	cluster		2.094	2.028	2.384	2.780	2.808	2.831
	periodic		2.060	2.019	2.521	2.798 (2.790)	2.811	2.865
$d(\text{Pd-C})$, Å	cluster	1.836	1.831	1.834	1.847	1.959	1.939	1.914
	periodic	1.857	1.845	1.839	1.843	1.958 (1.962)	1.949	1.915
$d(\text{C-O})$, Å	cluster	1.157	1.164	1.163	1.177	1.167	1.161	1.155
	periodic	1.162	1.164	1.166	1.176	1.164 (1.171)	1.162	1.160
$\alpha(\text{PdCO})$, °	cluster	180	180	180	157	147	180	180
	periodic	180	180	180	160	158 (149)	180	180
$\beta(\text{SPdC})$, ° ^c	cluster		0		39	32	0	46
	periodic		0		38	9 (43)	0	0
$D_c(\text{Pd-CO})$, eV	cluster ^d	2.40	2.73	2.58	1.47	0.79	0.72	1.30
	periodic	2.29	2.63	2.60	1.90	1.01 (0.98)	0.80	1.27
ω_0 , cm ⁻¹ ^e	cluster	2069	2062	2039	1947	1955	2039	2089
	periodic	2047	2061	2053	1966	2018 (1961)	2027	2049

^a PdCO⁺ results: $d(\text{Pd-C}) = 1.911$ Å; $d(\text{C-O}) = 1.133$ Å; $D_c(\text{Pd-CO}) = 2.20$ eV, $\omega_0 = 2206$ cm⁻¹; PdCO⁻ results: $d(\text{Pd-C}) = 1.849$ Å; $d(\text{C-O}) = 1.180$ Å; $D_c(\text{Pd-CO}) = 2.51$ eV, $\omega_0 = 1899$ cm⁻¹. ^b In parentheses are given the results of the 5×5 supercell calculations. ^c Angle of Pd-C bond with the surface normal. ^d BSSE corrected. ^e Scaling factors: cluster $f = 1.015$, periodic $f = 1.031$. ^f Experimental: $D_c(\text{Pd-CO}) \approx 1$ eV, $\omega_e = 2055$ cm⁻¹.

electron is localized in the center of the vacancy, Figure 2, and the defect has similar (although not identical) properties to those of the classical F⁺ defect.²⁴ In particular, in the periodic calculation the defect is neutral, at variance with the cluster model center which is positively charged.

A special emphasis in this study is given to the bonding and vibrational properties of CO adsorbed on a Pd atom deposited at various sites of the MgO surface. For this reason, it is important to comment on the properties of the free CO molecule as described at the PW-91 level by LCAO and plane wave approaches. The CO molecule has $r_e = 1.137$ Å and $\omega_0 = 2138$ cm⁻¹ according to the LCAO approach; $r_e = 1.146$ Å and $\omega_0 = 2104$ cm⁻¹ according to the plane wave method. The small differences can be due to the use of a pseudo-potential for C and O in the periodic approach, to differences in the basis sets, and to numerical accuracy. The computed values should be compared with the experimental $r_e = 1.13$ Å and $\omega_0 = 2170$ cm⁻¹ (this latter is the experimental harmonic frequency of CO; the anharmonic value is $\omega_e = 2143$ cm⁻¹).²⁶ Thus, both LCAO and plane wave approaches underestimate the stretching frequency of free CO. For this reason, we decided to apply a scaling factor to all computed frequencies; this scaling factor is $f = 2170/2138 = 1.015$ and $f = 2170/2104 = 1.031$ for cluster and periodic calculations, respectively.

A direct assessment of the reliability of our computed frequencies comes from the comparison with the existing experimental data for matrix-isolated Pd-CO, Pd-CO⁺, and PdCO⁻ complexes²⁷ (the plane wave calculations have been performed only for the neutral complex). The unsupported Pd-CO molecule is characterized by a relatively strong Pd-CO bond (≈ 2.3 eV) and by a vibrational frequency of 2069 cm⁻¹ (cluster) or 2047 cm⁻¹ (periodic), Table 1. The experimental value in Ne-matrix, 2056 cm⁻¹,²⁷ is between the two theoretical values. Pd-CO⁺ has a Pd-C bond, 1.911 Å, longer than in the neutral form, 1.836 Å, but has a similar binding energy, 2.20 eV; the computed vibrational frequency, 2206 cm⁻¹,²⁷ coincides with the experimental one. In PdCO⁻, the LCAO calculations give a bent molecule with a Pd-C-O bond angle of 154°, a C-O bond length of 1.180 Å, and a D_c of 2.51 eV;

**Figure 3.** Structure of a PdCO complex formed at a step site of the MgO surface.

the scaled vibrational frequency, 1899 cm⁻¹, is only 10 cm⁻¹ lower than the experimental one, 1909 cm⁻¹.²⁷ Thus, the scaled vibrational frequencies are within 20 cm⁻¹ to the measured one for isolated Pd-CO, Pd-CO⁺, and PdCO⁻ complexes.

3. Results and Discussion

3.1 The PdCO Surface Complex. The binding and vibrational properties of CO adsorbed on a Pd atom stabilized at regular and defect sites of the MgO surface are shown in Table 1. Since it is known from previous studies that metal atoms prefer to bind to the oxide anions of the MgO surface,²⁸ the analysis is restricted to these centers. The first line gives the shortest Pd-O distance before adding a CO molecule; the second line gives the same distance for the PdCO complex. In the following lines, we give the C-O optimal distance, the internal angle $\alpha(\text{PdCO})$, the tilt angle $\beta(\text{SPdC})$, where S represents surface, the Pd-CO binding energy, and the CO vibrational frequency, ω_0 , scaled as indicated in the previous section. First, we notice that embedded clusters with LCAO basis sets or supercells with plane waves give in general very similar results, providing a validation of both methods for this kind of system. PdCO complexes formed at oxide anions on terraces or steps (Figure 3) show Pd-C and C-O distances which agree to 0.01 Å, adsorption energies which are virtually identical, and vibrational frequencies which differ at most by 14 cm⁻¹. The properties of the complex on a divacancy are

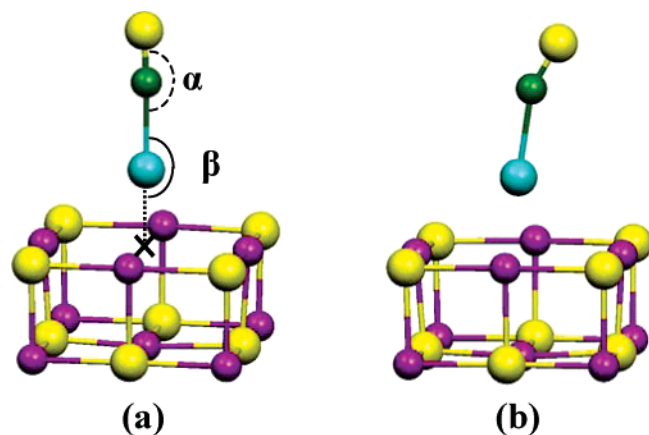


Figure 4. Structure of a PdCO complex formed on a neutral F_{5c} center: (a) normal (local minimum); (b) tilted (absolute minimum).

also similar in the two treatments (see, e.g., the internal and tilt angles which agree to 3° and the vibrational frequencies which differ by 19 cm^{-1}). However, the CO adsorption energy is considerably larger in the periodic calculation. We think that this is because the divacancy induces a large perturbation in the periodic potential of the MgO surface,^{11,12} so that long-range relaxation effects become important. These are properly included in the cluster model, where an isolated defect is considered, while much larger supercells could be necessary to get the same result in a periodic treatment.

This brings us to the important case of the F_{5c} center. Here, the CO molecule can assume two orientations, either normal to the surface or tilted, Figure 4. Both periodic and cluster calculations show that the tilted orientation is slightly preferred, in agreement with previous findings.^{8–10} By tilting the molecule, the binding energy goes from 0.72 to 0.79 eV in the cluster model and from 0.80 to about 1 eV in the periodic approach, Table 1. Part of the discrepancy is due to uncertainties in the BSSE correction which is applied to the LCAO calculations; on F_{5c} centers, this is 0.33 eV. The cluster and periodic binding energies obtained here with a PW exchange-correlation functional are a bit larger than the $D_e = 0.63\text{ eV}$ obtained at the B3LYP level in our previous studies.^{9,10} However, the quite good agreement between cluster and periodic calculations is obtained only if a 5×5 supercell is used: $\alpha(\text{PdCO})$ and the tilt angles are similar and the vibrational frequency is almost coincident, 1955 cm^{-1} (cluster) and 1961 cm^{-1} (periodic), Table 1. On the other hand, if we compare the geometries of F_{5c}/PdCO obtained with cluster and 4×4 supercell calculations (i.e., the same cell size used for the other sites), the comparison is not at all satisfactory. The PdCO internal angle and the tilt angles differ considerably; in particular, while in the cluster model the PdCO molecule is tilted by 32° from the surface normal, and the tilt is only 9° in the 4×4 supercell calculation. This has a large effect on the vibrational frequency which is predicted to be 1955 cm^{-1} in the LCAO method and 2018 cm^{-1} in the plane wave approach (the large red-shift induced by the tilting was noticed already in our previous work).⁸ For the normal orientation, the two approaches predict very similar frequencies, 2039 and 2027 cm^{-1} , respectively. Notice that the use of the 5×5 instead of the 4×4 supercell affects all properties except the adsorption energy which remains practically unchanged. This shows that the potential energy for Pd–CO bending is very flat, and the properties of the adsorbed complex depend markedly on the conformation assumed by the molecule. This provides a first important result of this study: without a detailed comparison

of cluster and supercell results, the insufficient size of the 4×4 supercell would have not been identified.

The case of the F_{5c}^+ center is somewhat simpler. Here, in fact, the complex is oriented along the surface normal, and the results of cluster and periodic calculations are surprisingly (and in part fortuitously) similar. One should not forget in fact that a positive charge is associated to the cluster defect while the corresponding periodic center is neutral. This reflects in particular in the value of the ω_0 which is 2049 cm^{-1} in the periodic approach and 2089 cm^{-1} in embedded cluster. The presence of a positive charge on the system results in a stronger electric field which shifts the CO frequency to higher values.²⁹ On the other hand, the geometrical parameters and the adsorption energy are practically identical with the two methods.

In short, the results reported in Table 1 represent a solid set of data to compare with experiment to establish the sites where most likely the Pd atoms are stabilized. They show that the embedding scheme used in the cluster model reproduces very well the solid-state effects; on the other hand, the supercells used are large enough to avoid mutual interaction of the defect sites or of the adsorbed molecules.

The binding of a Pd atom to the MgO surface varies considerably from site to site,⁶ being strongest on a neutral F_{5c} center (3.99 eV), followed by a divacancy and an F_{5c}^+ center, around 3 eV, by a step, 1.85 eV, and finally by a terrace site, 1.36 eV (these values, obtained with the PW-91 exchange-correlation functional and plane wave basis sets, are overestimated by 0.3–0.5 eV compared to other functionals such as the hybrid B3LYP). In the following, we try to identify possible trapping sites for the PdCO complexes on MgO thin films using as a reference the measured CO desorption energy for process 2, about 1 eV, and the ^{12}CO frequency measured above 270 K, 2055 cm^{-1} . We start from the terrace sites, although it has been demonstrated that the low diffusion barriers for Pd on MgO ($<0.4\text{ eV}$) make it unlikely that the metal atoms are stabilized at these sites except for very low temperatures.^{5,6,9} According to the calculations, CO is bound to a Pd/MgO(terrace) complex by about 2.7 eV and its vibrational frequency is $\approx 2060\text{ cm}^{-1}$, Table 1. Compared to the experimental results for MgO/Pd(CO), we notice that while the binding energy is almost 3 times larger than the measured one, the computed CO frequency is very close. The situation is similar for a step site: here the $D_e(\text{Pd}-\text{CO})$ is $\approx 2.6\text{ eV}$ and the scaled ω_0 is $\approx 2050\text{ cm}^{-1}$, Table 1. This clearly shows that Pd atoms adsorbed on terrace or step sites behave very similarly toward CO adsorption. On the other hand, even steps are not good trapping sites for Pd atoms since the diffusion barrier from these sites is not particularly high.⁹ Thus, it is unlikely that Pd atoms and Pd–CO complexes form at steps. The fact that the computed CO adsorption energy on Pd/MgO(terrace) or Pd/MgO(step) is 3 times larger than in the experiment rules out these sites as the sites where Pd atoms are bound at room temperature.

A particular attention has been given in the last couple of years to a particular kind of surface defect, the divacancy. The properties of Pd–CO complexes formed on these sites have never been analyzed before. Cluster and periodic calculations show a CO–Pd/MgO(divacancy) binding energy which is between 1.5 and 2 eV, Table 1, much higher than for reaction 2; the CO vibrational frequency, 1947 cm^{-1} (cluster) and 1966 cm^{-1} (periodic), is red-shifted by about 100 wavenumbers compared to the experimental one. On this basis, we can exclude that the Pd atoms deposited on MgO thin films are bound to divacancies. This does not mean that divacancies are not present on MgO surfaces. The experiments done to study the Pd–CO

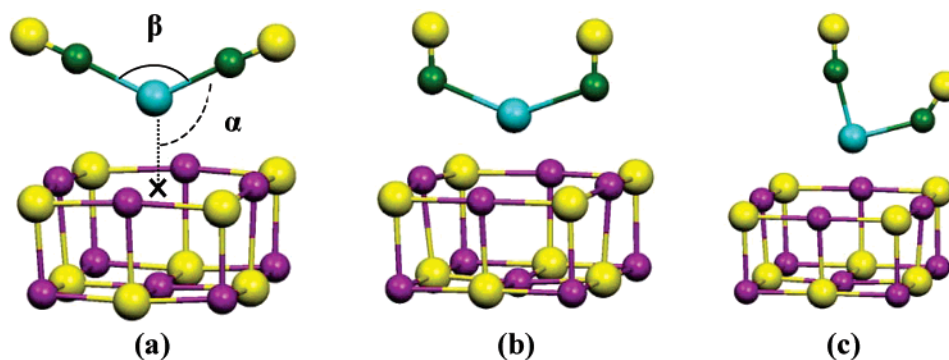


Figure 5. Various isomers of a $\text{Pd}(\text{CO})_2$ complex formed on a F_{5c} center on the MgO surface: (a) Sym1; (b) Sym2; (c) Asym. Sym1 corresponds also to the structure of the same complex on a F_{5c}^+ center.

bonding refer to MgO thin films,^{8,9} and it is possible that different kinds of defects are present on freshly cleaved MgO single crystals.¹³ There is now increasing evidence that differently prepared MgO surfaces can have different concentrations of the same defect.⁷

We consider now the F_{5c} center. The computed CO–Pd/MgO(F_{5c}) bonding is between 0.80 and 1 eV, Table 1, in close agreement with the experimentally measured desorption barrier for reaction 2. The CO vibrational frequency, however, 1955 cm^{-1} (cluster) and 1961 cm^{-1} (periodic), is completely off. This is true only when the molecule is bent;⁸ assuming a normal orientation, the predicted vibrational frequency is 2039 cm^{-1} (cluster) and 2027 cm^{-1} (periodic) and would be consistent with the experimental data. The fact that the bending of the PdCO complex implies a very flat potential leaves some doubts about the frequency values. Still, on the basis of a direct comparison of the vibrational frequencies for the most stable tilt structure, one should exclude the F_{5c} center as the site where the Pd atoms are bound.

The last case is that of the F_{5c}^+ center. Here, both approaches predict a Pd–CO binding energy of 1.3 eV, a bit overestimated with respect to experiment. A source of error for the cluster calculations comes from the BSSE correction, which is simple to apply for weakly distorted systems, less easy for systems which undergo structural distortion. Here, the classical counterpoise correction results in a small BSSE, 0.13 eV. Previous calculations performed at the B3LYP level and without BSSE correction gave for the same system a D_e of 0.82 eV.^{9,10} The C–O frequency computed with the cluster model, 2089 cm^{-1} , is blue-shifted by 40 cm^{-1} compared to the supercell model because the electric field associated to the charged defect interacts with the CO dipole moment. The supercell calculations show that the vibrational, geometrical, and energy properties of a Pd–CO complex formed on F_{5c} or “ F_{5c}^+ ” centers are similar (once more we notice that in a periodic calculation the only difference between F_{5c} and F_{5c}^+ centers is in the number of trapped electrons and not in the actual charge of the defect).

To summarize, the results reported in this section show that the bonding and vibrational properties of CO adsorbed on Pd atoms stabilized at F_{5c}^+ centers are in agreement with the experimental data. In the next section, we consider the formation of the $\text{Pd}(\text{CO})_2$ complexes on selected MgO sites.

3.2 The $\text{Pd}(\text{CO})_2$ Surface Complex. We first consider the formation of $\text{Pd}(\text{CO})_2$ complexes on a neutral F_{5c} center. As we will discuss in detail, the situation is rather complicated because of the existence of at least three different structural isomers, which however do not show up in all kind of calculations. The three minima are shown in Figure 5. Two of them exhibit a C_2 symmetry axis that will be identified as Sym1

and Sym2 in the following. The main difference between the two structures is that in Sym1 the CO molecules interact only with the Pd atom and form an almost linear Pd–C–O complex; in Sym2, the two CO molecules are bridge-bonded between Pd and a Mg ion at the border of the vacancy, and the Pd–C–O atoms form an angle of 111°. The third structure, asymmetric, has one CO bound nearly on top of Pd and the other close to a Mg ion at the border of the vacancy, see Figure 5c.

In Table 2, we give the main structural parameters of the various complexes: the shorter distance of the $\text{Pd}(\text{CO})_2$ complex from the surface, $d[\text{S}–\text{Pd}(\text{CO})_2]$, the Pd–C and C–O distances, the internal angle $\alpha(\text{CPdC})$, and the tilt angle $\beta(\text{SPdC})$. We also report the binding energy of CO to the $\text{Pd}(\text{CO})$ supported complex; this corresponds in the TDS experiment to the low-temperature peak, detachment of the first CO molecule, reaction 1. Finally, the vibrational frequencies of the symmetric and antisymmetric stretchings of the CO molecules are also given.

In embedded cluster calculations, there is only one minimum structure for the $\text{F}_{5c}/\text{Pd}(\text{CO})_2$ complex, Sym1, where the two CO molecules form an internal angle of about 120°, Table 2. All the attempts to locate other minima corresponding to Sym2 and Asym structures failed. In fact, geometry optimizations performed starting from these structures always arrive at the same Sym1 minimum shown in Figure 5. Therefore, we conclude that this is the absolute minimum of an isolated $\text{Pd}(\text{CO})_2$ complex on a neutral F_{5c} defect, in agreement with previous cluster calculations.^{8–10} This structure is found also in a periodic supercell calculation, with very similar geometrical parameters, provided that a 5×5 supercell is used, Table 2. In fact, using the smaller 4×4 supercell, the geometry optimization leads to two different structures with similar total energies. One corresponds to Sym2 and the other to Asym, Figure 5. The two structures differ in energy by 0.04 eV only and are found only when this supercell size is used. Curiously, while with the 5×5 supercell only the Sym1 structure is found, Sym1 is not even a local minimum with the 4×4 cell. This represents a warning for future studies of metal–CO complexes on the MgO surfaces with periodic supercells. Of course, given the very flat potential, one cannot exclude that the results of the optimizations are not fully converged, an aspect that to be investigated would require to run a short dynamics. The Sym1 structure is definitely more stable than Sym2 and Asym. In fact, the energy gain in adding a CO molecule to a $\text{F}_{5c}/\text{PdCO}$ surface complex is 1.05 eV while the corresponding value for Sym2 and Asym isomers is about 0.4 eV, Table 2. It is not clear why increasing the size of the supercell results in such a dramatic change in the structure of the global minimum, and we can only speculate that the presence of periodic boundary conditions, resulting in an unphysical concentration of defects in the

TABLE 2: Properties of a Pd(CO)₂ Complex Formed at F_{5c} and F_{5c}⁺ Defect Sites of the MgO(100) Surface: Cluster and Periodic Results^e

structure		F _{5c}			F _{5c} ⁺
		Sym1	Sym2	Asym	Sym1
cell dimensions	periodic	5 × 5	4 × 4	4 × 4	5 × 5
<i>d</i> [S–Pd(CO) ₂], Å	cluster	2.976	a	a	3.052
	periodic	2.923	2.790	2.663, 2.911	3.083
<i>D</i> (Pd–C), Å	cluster	1.942	a	a	1.939
	periodic	1.941	2.126	1.917, 2.048	1.933
<i>D</i> (C–O), Å	cluster	1.169	a	a	1.159
	periodic	1.168	1.180	1.165	1.163
α(CPdC), °	cluster	133	a	a	132
	periodic	120	139	88	126
β(xPdC), ° ^b	cluster	114	a	a	114
	periodic	120	111	167, 105	117
<i>D</i> _c [Pd(CO) ₂], eV	cluster	1.15 ^(c)	a	a	0.49 ^c
	periodic	1.05	0.41	0.37	1.26
ω ₀ , cm ^{−1} ^d	cluster	1956, 1984	a	a	2011, 2040
	periodic	1981, 2003	1871, 1906	1975, 2034	2008, 2036

^a No minimum was found for this structure. ^b Angle of Pd–C bond with the surface normal. ^c No BSSE correction. ^d Scaling factors: cluster *f* = 1.015, periodic *f* = 1.031. ^e Experimental: *D*_c[Pd(CO)₂ → Pd(CO) + CO] ≈ 0.6 eV, ω_e = 2055, 2090 cm^{−1}.

material, can give rise to some interaction between the adsorbed species. In the 4 × 4 supercell, Figure 1, the density of defects is of one vacancy every 32 surface atoms (3.1%), while in the 5 × 5 case (50 surface atoms) the concentration, 2%, is much closer to real experimental conditions (1–2%).^{8,9} On the other hand, the Asym structure described above has been reported previously by Abbet et al. on the basis of plane wave embedded cluster calculations,³⁰ suggesting a subtle dependence of the structure of M(CO)_{*n*} surface complexes on the details of the calculations.

As we mentioned above, in Sym1 (lowest isomer) the second CO is bound to F_{5c}/Pd(CO) by 1.15 eV (cluster) or 1.05 eV (periodic). This result is not coherent with the measured TDS spectra. In fact, the binding of the first and the second CO molecules to F_{5c}/Pd is comparable, around 1 eV, see Table 1 and Table 2. This should result in a single broad peak in the TDS spectrum and not in the double peak observed experimentally. In our previous cluster model calculations performed at the B3LYP level, we found a binding energy for the second CO molecule of 0.45 eV, a bit lower than for the first one, 0.63 eV. This led us to conclude that two distinct TDS peaks are predicted by the calculations.^{8–10} In view of the new results, however, one should admit that a difference of 0.18 eV is not large and does not account for the difference in the TDS peaks unless one assumes a significant underestimate of the F_{5c}/Pd–CO bond, 0.63 eV. Also, the vibrational frequencies of F_{5c}/Pd(CO)₂ do not fit with the experiment. Both ν_{asym} and ν_{sym}, 1956 cm^{−1} (cluster), 1981 cm^{−1} (periodic), and 1984 cm^{−1} (cluster) and 2003 cm^{−1} (periodic), Table 2, are nearly 100 cm^{−1} red-shifted compared to the experiment (2055 and 2090 cm^{−1}). This is consistent with the very long computed C–O distances, close to 1.17 Å, Table 2. This is a clear sign of a large back-donation of charge into the CO 2π* orbital because of the delocalization of the electrons trapped in the vacancy to the Pd(CO)₂ complex.

Let us assume now that Sym2 or Asym are the real structures of F_{5c}/Pd(CO)₂. In this case, the binding energy of the second CO molecule, ≈0.4 eV, Table 2, is a bit lower than the estimated one, 0.7 ± 0.1 eV, but at least two desorption peaks should occur in the TDS spectra, consistent with the experiment. On the other hand, the C–O stretching frequencies disagree considerably, in particular for the Sym2 structure where the difference compared to experiment is 180–200 cm^{−1}. For the Asym isomer, things are better since the difference between

theory and experiment is 60–80 cm^{−1} and could be due to an overestimate of the back-donation at the PW-DFT level. On the basis of this discussion, we have to conclude that also the results for the F_{5c}/Pd(CO)₂ surface complex present some discrepancies with respect to the measured desorption energies and vibrational frequencies. These discrepancies are largely connected to the multim minima nature of the potential energy surface and to the large change of bonding properties as function of the structural modification.

The other case considered is that of the F_{5c}⁺ center. As mentioned before, despite the notation used to identify this center which implies the presence of a positive charge, the characteristics are different in the cluster and periodic approaches. Despite these differences, the same minimum is found, similar to the Sym1 configuration found for F_{5c}, Figure 5a. The internal angle is a bit smaller than for the F_{5c} case, about 130°, but the geometric characteristics are similar in the two treatments. The C–O bond lengths are much shorter than for the neutral F_{5c} center, reflecting the presence of only one electron trapped in the vacancy, hence a smaller back-donation.

There is, however, a large difference in the two treatments related to the binding energy of the second CO: this is 0.49 eV in the cluster model and 1.26 eV in the periodic approach, Table 2. We do not have a simple rationalization for this result, which is clearly connected to the presence of a net positive charge in the cluster model. In this respect, while the periodic model of the F_{5c}⁺ center can describe several features of this center, it is clearly unable to reproduce all details of its electronic structure. The cluster result is consistent with the experiment since it gives a binding energy which is about one-half of that of the single CO; the periodic value is inconsistent, since it would imply the simultaneous desorption of the two CO molecules for temperatures well above RT (single TDS peak). The vibrational frequencies of F_{5c}⁺/Pd(CO)₂ in the cluster approach are 2011 and 2040 cm^{−1} and are quite similar to the periodic ones, 2008 and 2036 cm^{−1}, Table 2; they are 40–50 cm^{−1} lower than the experimental ones (2055 and 2090 cm^{−1}), a result which can be tentatively explained with the tendency of DFT to exaggerate back-donation for CO bound to metal atoms on F centers. Finally, the results obtained for the F_{5c}⁺ center with the shell model embedded cluster are qualitatively similar to those obtained at the B3LYP level using a simple point charges embedding.^{9,10}

4. Conclusions

We have studied with both embedded cluster and periodic approaches the properties of PdCO and Pd(CO)₂ complexes adsorbed on the surface of MgO with the aim to (a) improve the quality of the cluster calculations compared to previous studies,^{9,10} (b) verify the reliability of various properties (in particular vibrational frequencies) with the two methods, and (c) check the possible role of various point defects in stabilizing metal atoms at the surface of MgO. To this end, the computational results have been compared with TDS and FT-IR data on Pd(CO) and Pd(CO)₂ complexes on MgO thin films in UHV conditions.

The results can be summarized as follows:

Embedded cluster and periodic DFT calculations based on the same exchange-correlation functional (PW91) give in general very similar results for adsorption geometries, binding energies, and in particular vibrational frequencies. This is true for most sites, although some differences are found for special defects. This is the case of the divacancy, a defect center which induces a strong perturbation of the MgO surface potential, and of the F_{5c}⁺ center, an oxygen vacancy with a single trapped electron. For the divacancy, the largest difference is in the Pd–CO binding energy which differs in the two approaches by about 0.5 eV; however, the other properties are very similar, Table 1. For the F_{5c}⁺ center, a substantial difference is found in the F_{5c}⁺/Pd(CO)₂ → F_{5c}⁺/Pd(CO) + CO dissociation process, which has a very different cost in cluster and periodic calculations. This result must be ascribed to the different total charge of the defect in the two approaches. In this respect, it is rather surprising that all other properties computed for this center are very similar.

Periodic slab calculations show a dependence of some results on the size of the supercell. This is true in particular for Pd(CO)₂ complexes formed at neutral F_{5c} centers: different global minima are found using 4 × 4 or 5 × 5 supercells, suggesting a possible interaction among the surface complexes when smaller cells are used. This result has been found only because of the direct comparison with cluster calculations; convergence of the results versus supercell size is rarely systematically checked.

The results provide some clear indications for the interpretation of the experimental results and leave some questions open for future work. From the properties of PdCO complexes, one can safely exclude that sites such as surface oxide anions at terraces or steps are involved in the stabilization of these complexes, confirming our previous conclusions;^{8–10} even the MgO divacancies, never considered before in this context, are not good candidates as they provide bonding and vibrational properties of the PdCO complex that are not consistent with the measurements. The high-temperature peak observed in the TDS experiment is consistent only with the presence of Pd atoms bound at oxygen vacancies, either neutral or charged.^{8–10} The analysis of the corresponding vibrational frequency, however, seems to exclude the neutral F_{5c} centers as they induce large red-shifts in the C–O stretching frequency. In this respect, F_{5c}⁺/PdCO complexes are the best candidates to explain the high-temperature TDS and FT-IR data. The analysis of the properties of the Pd(CO)₂ complexes confirms this picture, although some uncertainties remain in the definition of the binding of the second CO molecule (low-temperature peak in TDS) and in the values of the computed frequencies which are 40–50 cm^{−1} too low compared to the experiment. These uncertainties leave space

for different interpretations of the experiment, like for instance the formation of Pd dimers formed at oxygen vacancies, an aspect that we plan to investigate in the near future.

Acknowledgment. This work has been supported by the European Union through the FP6 STRP project GSOMEN, by the Italian Ministry of University and Research (MIUR) through a Cofin 2003 project, by the Italian INFN through the initiative “Calcolo Parallelo”, and by the Deutsche Forschungsgesellschaft. We thank A. Shluger and P. Sushko (UCL London) for making available the Guess code.

References and Notes

- Freund, H.-J. *Surf. Sci.* **2002**, *500*, 271.
- Sanchez, A.; Abbet, S.; Heiz, U.; Schneider, W. D.; Ferrari, A. M.; Pacchioni, G.; Rösch, N. *J. Am. Chem. Soc.* **2000**, *122*, 3453.
- Sanchez, A.; Abbet, S.; Heiz, U.; Schneider, W. D.; Häkkinen, H.; Barnett, R. N.; Landmann, U. *J. Phys. Chem. A* **1999**, *103*, 9573.
- Bäumer, M.; Freund, H. J. *Prog. Surf. Sci.* **1999**, *61*, 127.
- Haas, G.; Menck, A.; Brune, H.; Barth, J. V.; Venables, J. A.; Kern, K. *Phys. Rev. B* **2000**, *61*, 11105.
- Giordano, L.; Di Valentin, C.; Goniakowski, J.; Pacchioni, G. *Phys. Rev. Lett.* **2004**, *92*, 096105.
- Pacchioni, G. *ChemPhysChem* **2003**, *4*, 1041.
- Abbet, S.; Riedo, E.; Brune, H.; Heiz, U.; Ferrari, A. M.; Giordano, L.; Pacchioni, G. *J. Am. Chem. Soc.* **2001**, *123*, 6172.
- Judai, K.; Abbet, S.; Wörz, A. S.; Heiz, U.; Giordano, L.; Pacchioni, G.; *J. Phys. Chem. B* **2003**, *107*, 9377.
- Giordano, L.; Del Vitto, A.; Pacchioni, G.; Ferrari, A. M. *Surf. Sci.* **2003**, *540*, 63.
- Ojamäe, L.; Pisani, C. *J. Chem. Phys.* **1998**, *109*, 10984.
- Ricci, D.; Pacchioni, G.; Sushko, P. V.; Shluger, A. L. *J. Chem. Phys.* **2002**, *117*, 2844.
- Barth, C.; Henry, C. R. *Phys. Rev. Lett.* **2003**, *91*, 196102.
- Bogicevic, A.; Jennison, D. R. *Surf. Sci.* **1999**, *437*, L741.
- Sushko, P. V.; Shluger, A. L.; Baetzold, R. C.; Catlow, C. R. A. *J. Phys.: Condens. Matter* **2000**, *12*, 8257.
- Kresse, G.; Hafner, J. *Phys. Rev. B* **1993**, *47*, 558. Kresse, G.; Furthmüller, J. *Phys. Rev. B* **1996**, *54*, 11169.
- Perdew, J. P.; Chevary, J. A.; Vosko, S. H.; Jackson, K. A.; Pederson, M. R.; Singh, D. J.; Fiolhais, C. *Phys. Rev. B* **1992**, *46*, 6671.
- Stevens, W. J.; Basch, H.; Krauss, M. *J. Chem. Phys.* **1984**, *81*, 6026.
- Susko, P. V.; Shluger, A. L.; Catlow, C. R. A. *Surf. Sci.* **2000**, *450*, 153.
- Frisch, M. J.; Trucks, G. W.; Schlegel, H. B.; Scuseria, G. E.; Robb, M. A.; Cheesman, J. R.; Zakrzewski, V. G.; Montgomery, J. A.; Stratmann, R. E.; Burant, J. C.; Dapprich, S.; Millam, J. M.; Daniels, A. D.; Kudin, K. N.; Strain, M. C.; Farkas, O.; Tomasi, J.; Barone, V.; Cossi, M.; Cammi, R.; Mennucci, B.; Pomelli, C.; Adamo, C.; Clifford, S.; Ochterski, J.; Peterson, G. A.; Ayala, P. Y.; Cui, Q.; Morokuma, K.; Malick, D. K.; Rabuck, A. D.; Raghavachari, K.; Foresman, J. B.; Cioslowski, J.; Ortiz, J. V.; Stefanov, B. B.; Liu, G.; Liashenko, A.; Piskorz, P.; Komaromi, I.; Gomperts, R.; Martin, R. L.; Fox, D. J.; Keith, T.; Al-Laham, M. A.; Peng, C. Y.; Nanayakkara, A.; Gonzalez, C.; Challacombe, M.; Gill, P. M. W.; Johnson, B. G.; Chen, W.; Wong, M. W.; Andres, J. L.; Head-Gordon, M.; Repogle, E. S.; Pople, J. A. *Gaussian 98*, Revision A.6; Gaussian Inc.: Pittsburgh, PA, 1998.
- Hay, P. J.; Wadt, W. R. *J. Chem. Phys.* **1985**, *82*, 299.
- Boys, S. F.; Bernardi, F. *Mol. Phys.* **1970**, *19*, 553.
- Vanderbilt, D. *Phys. Rev. B* **1990**, *41*, 7892.
- Ménétrey, M.; Markovits, A.; Minot, C.; Del Vitto, A.; Pacchioni, G. *Surf. Sci.* **2004**, *549*, 294.
- Hammer, B. personal communication, 2004.
- Herzberg, G. *Molecular Spectra and Molecular Structure*; Van Nostrand: Princeton, New York, 1950; Vol. 1.
- Liang, B.; Zhou, M.; Andrews, L. *J. Phys. Chem. A* **2000**, *104*, 3905.
- Yudanov, I.; Pacchioni, G.; Neyman, K.; Rösch, N. *J. Phys. Chem.* **1997**, *101*, 2786.
- Pacchioni, G.; Cogliandro, G.; Bagus, P. S. *Int. J. Quantum Chem.* **1992**, *42*, 1115.
- Abbet, S.; Heiz, U.; Häkkinen, H.; Landman, U. *Phys. Rev. Lett.* **2001**, *86*, 5950.